Non-Destructive Testing for Evaluation of Defects and Interfaces in Metal-Carbon Fiber Reinforced Polymer-Hybrids

H.-G. Herrmann, M. Schwarz, J. Summa, F. Grossmann

Abstract—In this work, different non-destructive testing methods for the characterization of defects and interfaces are presented. It is shown that, by means of active thermography, defects in the interface and in the carbon fiber reinforced polymer (CFRP) itself can be detected and determined. The bonding of metal and thermoplastic can be characterized very well by ultrasonic testing with electromagnetic acoustic transducers (EMAT). Mechanical testing is combined with passive thermography to correlate mechanical values with the defect-size. There is also a comparison between active and passive thermography. Mechanical testing shows the influence of different defects. Furthermore, a correlation of defect-size and loading to rupture was performed.

Keywords—Defect evaluation, EMAT, mechanical testing, thermography.

I. INTRODUCTION

IN contrast to many high load-bearing hybrid-joints applicable in aerospace, the introduced concept is suitable for cost-optimized series-production, e. g. for automotive applications. The planar hybrid-joint is achieved by inserting a metallic structure with a thermoplastic injection-molded coating of optimized geometry between the CFRP laminate-plies within the RTM-process.

Although a lot of investigations had been carried out in the past decades on each of the involved materials [1]-[4], the mechanical behavior as well as the damage mechanisms of metal to CFRP hybrid-joints are barely known. Most of the state of the art works focused on the fatigue behavior of adhesively bonded CFRP-laminates. Thereby, cohesive failure was found to occur most-likely in the adhesive, which is a typical failure pattern related to slow fatigue crack growth [5]. Furthermore, it was reported that delamination growth within the CFRP-laminate is strongly promoted by penetrative reinforcements [6]. Since the metal-CFRP-hybrid investigated in this work penetrates the CFRP-laminate, competing damage mechanisms of cohesive failure and delamination growth are expected to occur. However, it is the main objective of this work to focus non-destructive testing (NDT) on the bonding

H.-G. Herrmann is with the Chair for Lightweight Systems, University of Saarland and with the IZFP Fraunhofer Institute for Nondestructive Testing, Campus E3.1, 66123 Saarbrücken, Germany (corresponding author, e-mail: hans-georg.herrmann@izfp.fraunhofer.de).

M. Schwarz, J. Summa, and F. Grossmann are with the Chair for Lightweight Systems, University of Saarland, Campus E3.1, 66123 Saarbrücken, Germany (e-mail: Michael.schwarz@izfp-extern.fraunhofer.de, Jannik.summa@izfp-extern.fraunhofer.de, Felix.grossmann@izfp-extern.fraunhofer.de).

zone between the components, which depicts the place of structural weakening due to gradient mechanical properties.

Since imperfections strongly affect the laminate properties [2], defects that arise due to the manufacturing have to be considered. Hence, a comparative study on quasi-static tensile tests is presented. Hereby, the influence of pre-selected defects, i.e. pleat, delamination, and 10° fiber misalignment, is evaluated by means of the maximum load bearing capability and the energy absorption.

II. HYBRID JOINT WITH THERMOPLASTIC INTERLAYER

By comparing metal and CFRP to a hybrid component, there is always the problem of different stiffness. To reduce this gap in stiffness between the CFRP and the metal component and to ensure that there will not be any corrosion to occur, a thermoplastic is inserted between the metal and the CFRP.

The CFRP component is a 3K plain weave with 30 vol.% of carbon fiber embedded in an epoxy matrix and is made up of four layers [0°/90°, ±45°]. The thermoplastic is a Polypropylene (PP) and the metal is an EN AW-6082 (AlSi1MgMn) aluminum.

Fig. 1 (a) shows the geometric parameters of the 4-mm thick aluminum insert encased with a 2-mm thick PP layer. Fig. 1 (b) illustrates the positioning of the insert between the middle plies of the 1-mm thick CFRP-laminate.
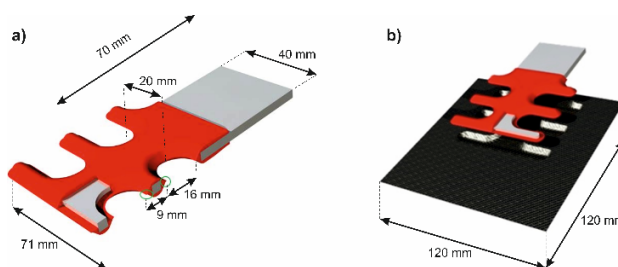

Fig. 1 a) Geometric specification of the aluminum-PP insert, b) insert positioned between the CFRP-laminate [7]

III. THEORY ON THERMOGRAPHY

In general, there are two different methods of measurement in thermography, passive and active thermography.

For active thermography, an external excitation is needed to achieve a thermal contrast in the specimen. As excitation source ultrasonic, eddy current, laser, halogen lamps or flash generators can be used. In this work, flash light with 3.2 kJ

power is used, because it is a very fast and contactless method. Furthermore, the measured data are captured as images and can be used for a qualitative assessment of inhomogeneities without an additional data or image processing.

After the specimen is excited, an infrared camera with Stirling cooler captures the thermal radiation, as depicted in Fig. 2. The used infrared camera is a so-called Dualband camera which is able to capture the radiation of midwave (4.4 - 5.2 µm) and longwave (7.8 - 8.8 µm) infrared. The detector type of the camera is a focal plane array (FPA) Quantum Well Infrared Photodetector (QWIP) with a lateral resolution of 384x288 pixels. The temperature sensitivity is 25 mK and the pixel pitch is 40 µm. Furthermore, the camera is able to record a frame rate of 300 Hz [8].
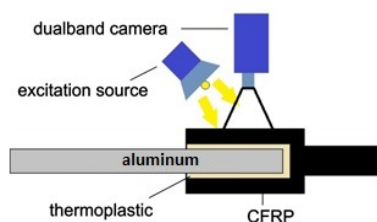

Fig. 2 Measurement configuration of thermography testing [9]

The surface of any object whose temperature is above absolute zero radiates energy in form of infrared radiation [10]. As the emitted radiation is a function of temperature, it can be concluded that with a higher temperature the radiant power increases. To capture this radiation of a specimen by an infrared camera, it has to be guaranteed that the emissivity is high enough to get sufficient radiation [11]. Since normal specimens do not act like blackbodies, it could be necessary to color the surface black to decrease reflection processes. Because the emissivity of CFRP is close to 1, a coloring is not necessary. While recording the radiation, defects act like thermal barriers and are depicted as bright areas in the infrared image.

In addition to the analysis of the radiation during the cooling process, the radiation can also be recorded using the lock-in method while the specimen is heated up. In this work, the intensity of eddy current is modulated by a square signal while the infrared camera captures the radiation at the specimen's surface. This method is called induction-lock-in thermography (ILT) and is used because of its short inspection time and high proof sensitivity [12]. From the measured image sequence, an amplitude image and a phase image can be calculated using Fourier transformation. In a phase image, some disruptive effects that are caused by e.g. inhomogeneous excitation are decreased. To vary the depth of thermal penetration in the material, the modulation frequency can be changed (cf. (1)).

$$\mu = \sqrt{\frac{\alpha}{\pi \cdot f}} \qquad (1)$$

where μ: depth of thermal penetration [m], α: thermal

diffusivity $[\frac{m^2}{s}]$ and f: modulation frequency $[\frac{1}{s}]$

In contrast to active thermography techniques, passive thermography does not need any external excitation methods. As deformation processes and friction cause internal heat dissipation within the material, passive thermography can be applied for *in situ* damage monitoring. Temperature variations caused by internal heat dissipation can be described as a superposition of thermoelastic temperature variation ΔT_{el}, heat dissipation ΔT_{diss} and heat exchange with the environment ΔT_{loss}, see (2) [13]:

$$\Delta T(t) = T(t) - T_0 = \Delta T_{el}(t) + \Delta T_{diss}(t) + \Delta T_{loss}(t) \quad (2)$$

where ΔT: total temperature change [K], T_0: absolute reference temperature [K] at t=0.

Commonly applied methods are mechanical induced dissipated heat analysis (MIDA) or thermal stress analysis (TSA), which enable the identification of weak spots or defects by local temperature hot spots during mechanical testing.

By using thermography as NDT method, there is the possibility to detect defects in the CFRP-structure and at the interface of the hybrid. Furthermore, the sample can be characterized before, after, and during mechanical testing by active and passive thermography. Finally, the maximum information on the defects and the damaging processes that follow by consequence is achieved by correlating the different thermography methods.

IV. Shear Horizontal Guided Waves (SH-Waves)

In addition to thermographic methods, shear horizontal guided waves (SH-waves) are used to characterize the hybrid structure. SH-waves are a special form of ultrasonic waves propagating in plates. They are characterized by an oscillation of the lattice atoms in the plane parallel to the surface and perpendicular to the direction of propagation. Provided that the oscillation is in the same dimension as the ultrasonic wavelength, oscillation occurs in the entire thickness of the plate. This vibration spreads along the whole plate until it is reflected at sharp edges, for example at the end of the plate.

SH-waves are used to investigate metallic structures [14], but they are also proved to be promising for the application on adhesive bonded samples consisting of two metallic plates [15], [16] as well as polymer/composite parts [17], [18].

In this work, SH-waves will be excited with EMAT with a frequency of 800 kHz. In contrast to normally used piezoelectric transducers, the advantage of EMAT is that no couplant medium is needed [19]. Furthermore, it is a contactless method. As this method is used to characterize, inter alia, adhesive bonded samples [16] further advantages arise. Due to the fact that the waves propagate along the whole surface and because of their long-range capability, it is possible to excite waves apart of the join. At the same time, inaccessible locations can be reached.

In case of the aforementioned hybrid structure, the interface between the aluminum and the polymer can be investigated by

using surface acoustic waves. Especially, the quality of the connection between the two components and also defects can be characterized.

V. Experimental Setup

Prior to mechanical testing, the hybrid-joints are subjected to active thermography. Thereby, the defects, which were artificially implemented into the CFRP-laminate within the RTM process, are characterized in terms of type, size, and location.

After defect characterization with active thermography, mechanical testing with passive thermography damage monitoring is carried out. The specimens were mounted with side-action screw-grips with a clamping length of 25 mm on both sides. According to DIN EN ISO 527, the tensile tests are driven displacement controlled with 2 mm/min cross-head speed.

The mechanical testing was complemented with an InfraTec VarioCam® HD Head bolometer camera with a resolution of 1024 x 768 pixels, spectral sensitivity in the range of 7.5 to 14 μm and a temperature resolution below 0.05 K (at T= 303.15 K). Thereby, thermography and mechanical testing data were synchronized by triggering the bolometer camera at t = 0 with 3 Hz image acquisition. Thus, changes in the IR images could be attributed to events in force-displacement diagrams at corresponding times.

Thermoelastic stress analysis was carried out under sinusoidal loading with 5 Hz and 0.2 mm amplitude, whereas the camera acquisition was driven with 30 Hz.

VI. Results

As mentioned in the introduction the results of active and passive thermography are shown and combined in this chapter. Furthermore SH-wave-measurements are used to enhance the characterization of the hybrid structure.

A. Active Thermography

By using active thermography, hybrid samples are checked for defects. These measurements are performed after a quasistatic tensile test. In Fig. 3, a hybrid sample is shown 7 ms after flash excitation. In the infrared image, a bright area between the lower and the middle arm can be seen. This bright area represents an artificial induced pleat defect in the upper CFRP-layer. Additional impairment is not detectable at this time after flash excitation.

In Fig. 4, the same sample as in Fig. 3 is shown. The infrared image has been recorded 1.4 seconds after flash excitation. In addition to the pleat defect, a bright area around the aluminum insert can be detected. This bright area can be characterized as delamination between CFRP and thermoplastic.

Besides defects in the CFRP-layers, defects at the interface of CFRP and thermoplastic can be characterized. This fact is very important, since this interface is the most important part for the force transmission in the hybrid structure.
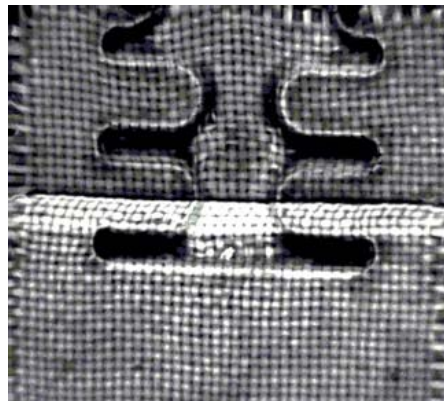

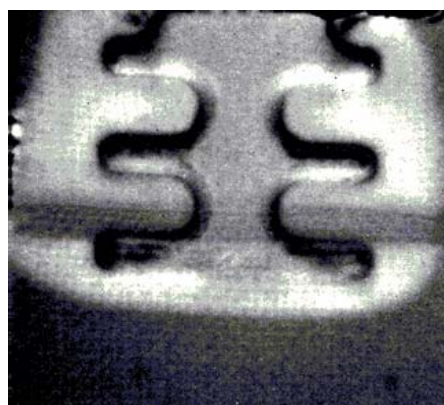Fig. 3 Hybrid sample with artificial induced pleat defect, 7 ms after flash excitation

Fig. 4 Hybrid sample with artificial induced pleat defect, 1.4 seconds after flash excitation

B. In Situ Damage Monitoring with Passive Thermography

First of all, the damage detection with passive thermography was improved by data optimization. This was performed by calculating the differential T-image, which refers to the initial sample temperature before loading $T(t=0)$.

The damage evolution of the aluminum-CFRP hybrid joints was investigated by means of tensile tests with passive thermography. A representative tensile test of a specimen with a pleat is shown in Fig. 5. The corresponding measures with passive thermography are given in Fig. 6.

In the first stage linear behavior was found, which turns to nonlinear behavior above 0.25 mm. Subsequently, several discontinuities are found until the maximum load bearing capability is reached. The maximum value is 6.3 kN located at a displacement of 1.25 mm. After this point, the damage proceeds in a stick-slip manner until the load bearing capability vanishes. The events of damage propagation can easily be identified applying passive thermography (Fig. 6), as spontaneous heating accompanies the characteristic stick-slip behavior. Thus, especially new generated fracture surfaces are well visible. This technique provides information on the damage mechanism and the dimension of the damage. Furthermore, this information can be correlated with mechanical quantities from the force-displacement curve. As

already mentioned, the force-displacement diagram shows several discontinuities before the maximum load is reached. These can be attributed to non-critical damages. One of these is depicted in Fig. 6 (a), emerging beneath the lowest arm of the insert. With this onset of damage, the debonding between PP and CFRP starts at the lowest point of the joining zone. Subsequently radial mode-I delamination propagates (Fig. 6(b) and (c)) until the fir tree formed insert is fully delaminated from the CFRP-laminate. This is accompanied by a vanishing load bearing capability (Fig. 6 (d)). This indicates firstly, that mode-I delamination is induced due to a pull-out effect of the insert, which is in good agreement with the observations of [6]. Secondly the damage somehow starts at the lower end of the insert. Therefore, additional investigations are carried out on the damage initiation using the thermoelastic stress analysis (Fig. 7).
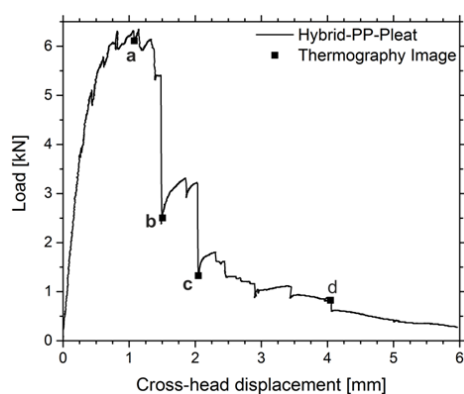

Fig. 6 Thermography images at displacements of (a) 0.98 mm, (b) 1.89 mm, (c) 2.21 mm, (d) 3.06 mm; ΔT-contrast

According to (1), the T-amplitude can be directly correlated to the acting stress. Hence, a stress concentration is located at the bright areas, which is underneath the insert. This measurement is in perfect agreement with the observation that the debonding between the PP and the CFRP starts in this region.

By comparing active and passive thermography, it is possible to characterize the state of the hybrid sample before, while, and after the mechanical testing. Through the passive thermography statements about failure behavior can be made. By analyzing active thermography results, we additionally get information about the defect size and defect depth.

Fig. 5 Force-displacement diagram of a defect-free hybrid-joint, dots: times of the four thermography images shown in the subsequent figure
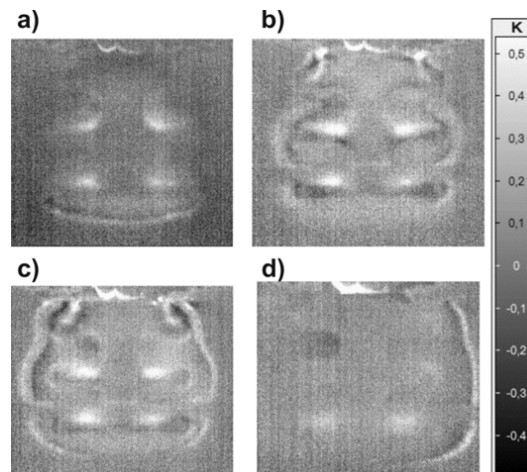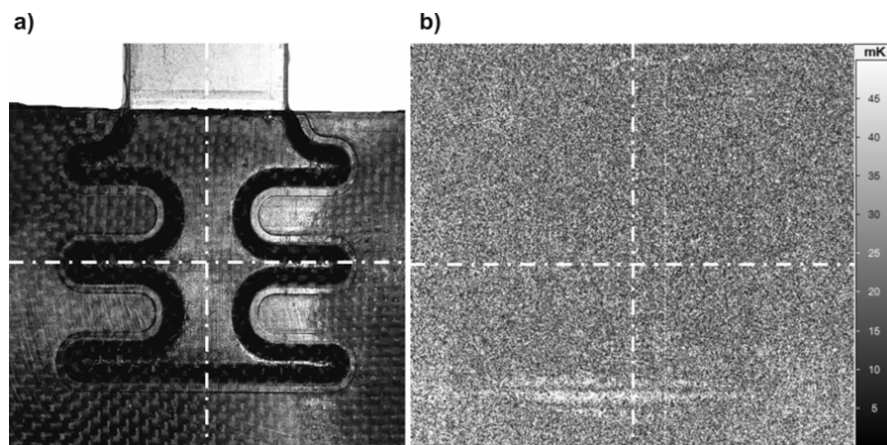

Fig. 7 (a) Position of the investigated specimen, (b) amplitude-image of lock-in thermography, with highlighted maximum and average values of T-amplitude

C. Shear Horizontal Guided Waves (SH-Waves)

In addition to thermography also ultrasonic testing is used to characterize the hybrid-joint. In cases of plate-like specimens the propagation of ultrasonic pulses occurs as shown in Fig. 8. The first signal is the direct signal between the transmitter and the receiver. The second and third signals are the reflection at the near and the far end of the plate, respectively. By moving the transmitter and the receiver, it is ensured that the signals do not overlap. However, in Fig. 9, only the first signal is separated and can be easily detected,

whereas all other signals overlap so that they cannot be clearly identified. Nevertheless, the condition of the aluminum insert can be characterized. In Fig. 9, the signal of an aluminum insert with thermoplastic (black line) is compared to the signal of an aluminum insert without thermoplastic (gray line). The signal of the aluminum insert with thermoplastic is significantly reduced. This can be seen especially at 70 μs and 85 μs. This indicates that the bonding to a thermoplastic causes an attenuation of the ultrasonic signal.
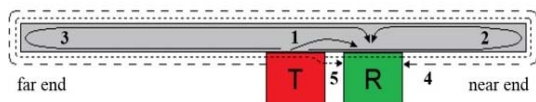

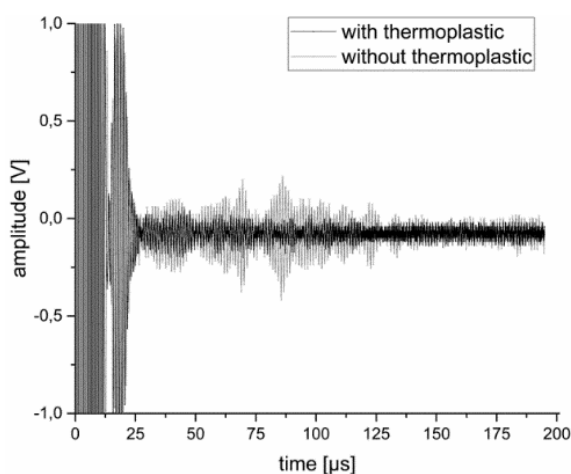Fig. 8 Propagation of ultrasonic pulses resulting in different signals [20]

Fig. 9 Amplitude of ultrasonic signal in aluminum insert with and without a thermoplastic component

D. Influence of Defects

In order to evaluate the influence of the pre-selected defects, the specimens with and without these defects were subjected to tensile tests. Fig. 10 summarizes the results of tensile tests on hybrid-joints with pleat, delamination and 10° misalignment as well as defect-free ones.

Fig. 10 shows that the qualitative mechanical response remains the same, regardless of the defect-types. All samples fail in a stick-slip manner accompanied by a decrease of the bearable load. Thereby, several drops of the measured load occur, which can be attributed to delamination growth (see Figs. 5 and 6). Additionally, average-value curves are depicted in Fig. 11, as mechanical quantities are more comparable. Note that each curve is built out of five single tensile tests.

The average-value curves start to diverge at approximately 0.25 mm. From there, various differences are visible. One major effect of the implemented defects is the achieved maximum load, prior to rupture. Focusing on the proceeding damage, the relations between the curves remain similar. This tendency gets clearer as the results on the tensile tests can also be analyzed statistically by means of mechanical quantities, as shown in Fig. 12.
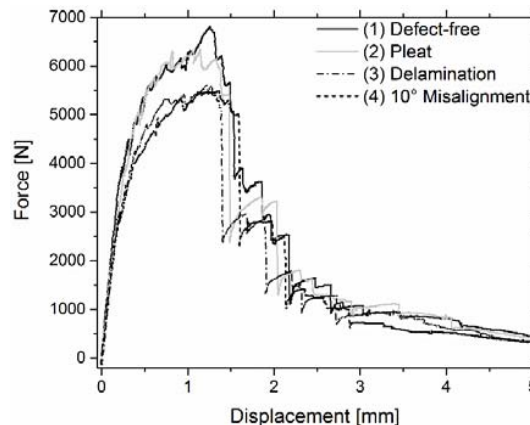

Fig. 10 Force-displacement diagram of uniaxial tensile tests (2 mm/min cross-head speed) with hybrid joints containing different defect types
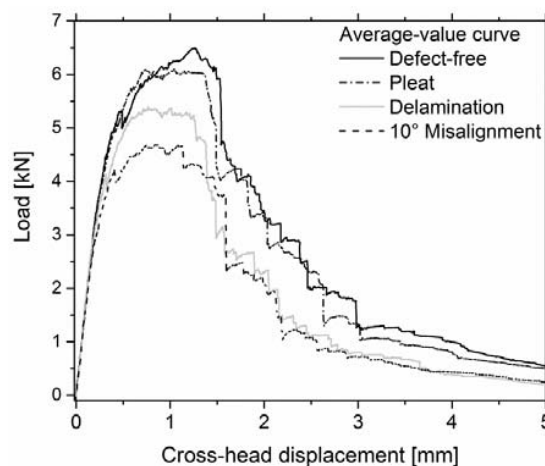

Fig. 11 Average-value curves of uniaxial tensile tests (2 mm/min cross-head speed) with hybrid joints containing different defect types
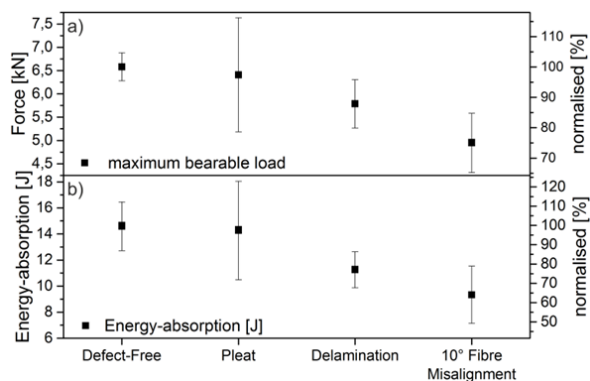

Fig. 12 Statistical analysis of a) load bearing capability (force of rupture), b) energy absorption

It can be found that the maximum load bearing capability hardly decreases due to the pleat. In contrast, the 10° misalignment causes a decrease of 25 % and delamination of 20 %. Likewise, the energy absorption (Fig. 12 (b)) shows the

same tendency as the load bearing capability. The decrease caused by the pleat is neglectable, whereas the energy absorption drops down below 80 % in presence of a delamination. Even higher affection is seen in case of the 10° misalignment reaching 65%.

E. Correlation of Loading Force and the Defect-Size

By comparing mechanical characteristics with thermographic results of defects, we are able to assess the state of the hybrid joint. In Fig. 13, a correlation of the loading force and the angle of misalignment has been performed. It can be noted that, by increasing the angle of the misalignment defect, the maximum force decreases.
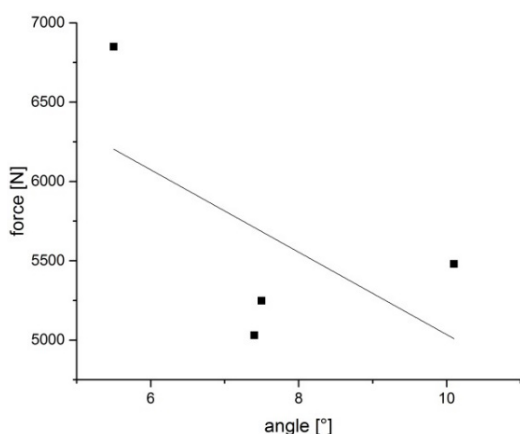

Fig. 13 Correlation of force and angle of misalignment

In Fig. 14, a correlation of the force and the area of a pleat is shown. It is expected that, by increasing the pleat-defect, the force decreases. But as depicted in Fig. 14, the force increases while the area of the pleat is increased. This circumstance can be explained by looking at Fig. 3. The pleat defect is above an aluminum arm of the insert which is the location for the most stress to occur. Due to the pleat, the area to relieve the tension increases. Furthermore, we get an additional layer which enforces the hybrid.
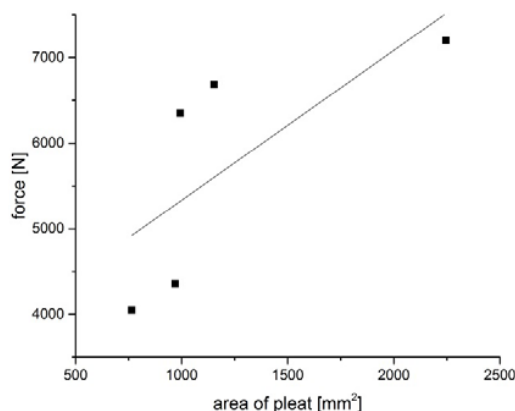

Fig. 14 Correlation of force and area of pleat

VII. Conclusion

In this work, different NDT methods are shown, which enabled the characterization and evaluation of defects and interfaces in an aluminum-CFRP hybrid.

The quality of the hybrid-joints was evaluated prior to mechanical loading. Hereby, active thermography measurements of the specimens with imperfections have shown high lateral resolution and in depth. Hence, all defects were characterized in terms of type, size and position. Additionally, the thermoplastic-CFRP interface was assessed in terms of location and condition.

Thermoelastic stress analysis with passive thermography enabled to localize stress concentrations in the hybrid-joint. In subsequent tensile tests the damage was found to initialize at this particular stress concentration. Moreover, the application of in situ passive thermography whilst mechanical testing enabled to monitor the complete damage process, from initiation to final rupture. This technique provides the correlation of each thermography-image with its corresponding point in the load-displacement curve. So, the present observations revealed that delamination growth at the thermoplastic-CFRP interface was the predominant damage-mechanism. On the downside, this technique provides no information on depth. This is counteracted by active thermography measurements, as the exact size and position (depth) of the mechanical induced delamination is characterized. Finally, the lateral sizes of the delaminations, determined with active and passive thermography, are in well agreement.

Using EMAT, we are able to characterize the state of the interface between the aluminum and the thermoplastic. It is shown that, through the thermoplastic component, the ultrasonic signal is dumped. In consequence, in further works, the art of the interface will be characterized in situ during mechanical testing.

Ultimately, the combination of active and passive in situ thermography results in a complete overview of specimen failure. Thereby, the in situ technique enables the correlation of material processes and mechanical quantities, whereas active thermography provides full volume information on defects and damages.

The long-term target is to determine the damage size and location within the specimen by active thermography and to predict the outlasting lifetime until rupture. One possible approach is to build a defect-failure master curve by correlating the load of damage propagation against the corresponding area of delamination.

REFERENCES

[1] W. J. Cantwell and J. Morton, "the significance of damage and defects and their detection in composite materials: a review", Journal of Strain Analysis, 27 (1), 1992.

[2] K. Senthil et al., "Defects in composite structures: Its effects and prediction methods- A comprehensive review", Composite Structures, 106, p. 139-149, 2013.

[3] E. S. Greenhalgh and M. J. Hiley, "Fractography of Polymer Composites: Current status and Future issues", London Imperial College, 2015.

[4] O. Al-Khudairi et al., "Characterising mode I/mode II fatigue delamination growth in unidirectional fibre reinforced polymer laminates", Materials and Design, 66, p. 93-102, 2015.

[5] J. P. Casas-Rodriguez, I. A. Ashcrof and V. V. Silberschmidt, "Delamination in adhesively bonded CFRP joints: Standard fatigue, impact fatigue and intermittent impact", Composites Science and Technology, 68, p 2401-2409, 2008.

[6] P. N. Parkes et al., "Static strength of metal-composite joints with penetrative reinforcement", Composite Structures, 118, p. 250-256, 2014.

[7] J. Summa, M. Schwarz and H.-G. Herrmann, "Evaluating the Severity of Defects in a metal to CFRP hybrid-joint with in situ passive thermography damage monitoring", Proceedings 5th International Conference on Integrity, Reliability & Failure, Porto, p. 117-126, 2016.

[8] Thermosensorik. Operating Manual – Infrared Camera Head QWIP 384 Dualband (2009).

[9] M. Schwarz, J. Summa and H.-G. Herrmann, "Characterizing Metal - CFRP Hybrid Structures by Nondestructive Testing Methods", Proceedings 5th International Conference on Integrity, Reliability & Failure, IRF Porto, p. 127-136, 2016.

[10] C. Meola, "Origin and Theory of Infrared Thermography", Infrared Thermography: Recent Advances and Future Trends, Meola, C. (Ed.), Bentham Science: New York, NY, USA (2012).

[11] X. P. V. Maldague, *Theory and Practice of Infrared Technology for Nondestructive Testing*. John Wiley & Sons, Inc., 15-32 (2001).

[12] V. Carl and G. Zenzinger, "Automatische Rissprüfung mit induktiv angeregter Thermografie", DGZfP-Berichtsband 94, (2009).

[13] H. Rösner, U. Netzelmann, J. Hoffmann, W. Karpen, V. Kramb and N. Meyendorf, *Thermographic Materials Characterization*. Springer 246-285 (2004).

[14] P. Petcher, M. D. G. Potter and S. Dixon, "A new electromagnetic acoustic transducer (EMAT) design for operation on rail", NDT&E International 65, 1-7 (2014).

[15] K. Arun, R. Dhayalan, K. Balasubramaniam, B. Maxfield, P. Peres and D. Barnoncel, "An EMAT-based shear horizontal (SH) wave technique for adhesive bond inspection", Proceedings of the National Seminar and Exhibition on NDE (2011).

[16] M. Castaings, "SH ultrasonic guided waves for the evaluation of interfacial adhesion", Ultrasonics 54, 1760-1775 (2014).

[17] B. Le Crom and M. Castaings, "Shear horizontal guided wave modes to infer the shear stiffness of adhesive bond layers", The Journal of the Acoustical Society of America 127(4), 2220-2230 (2010).

[18] P. Pérès, D. Barnoncel, K. Balasubramaniam and M. Castaings, "New Experimental Investigations Of Adhesive Bonds With Ultrasonic SH Guided Waves", 18th International Conference on Composite Materials (2011).

[19] H.-J. Salzburger, F. Niese and G. Dobmann, "EMAT pipe inspection with guided waves", Welding in the world, 56(5-6), 35-43 (2012).

[20] S. Quirin, S. Neuhaus and H.-G. Herrmann, "Testing Ultrasonic SH waves to estimate the quality of adhesive bonds in small hybrid structures", Proceedings of Euro Hybrid Materials and Structures, Kaiserslautern, Germany (2016).